HHS Public Access

Author manuscript

Photochem Photobiol. Author manuscript; available in PMC 2015 September 14.

Published in final edited form as:

Photochem Photobiol. 1997 March ; 65(3): 422–426.

The Role of Subcellular Localization in Initiation of Apoptosis by Photodynamic Therapy

David Kessel[1,*], **Yu Luo**[1], **Yongqi Deng**[2], and **C. K. Chang**[2]

[1]Department of Pharmacology, WSU School of Medicine and Department of Chemistry, Michigan State University, Detroit, MI, USA

[2]Department of Chemistry, Michigan State University, East Lansing, MI, USA

Abstract

Rapid initiation of apoptosis can be induced by photodynamic therapy, depending on the cell line and sensitizer employed. In this study, we evaluated the photodynamic responses to two structurally related photosensitizing agents, using the P388 murine leukemia cell line in culture. Photodamage mediated by tin etiopurpurin involved lysosomes and mitochondria and yielded a rapid apoptotic response; apoptotic nuclei were observed within 60 min after PDT. A drug analog, tin octaethylpurpurin amidine, targeted lysosomes, mitochondria and cell membranes; apoptotic nuclei were not observed until 24 h after PDT. These results, together with other recent reports, are consistent with the hypothesis that membrane photodamage can delay or prevent an apoptotic response to PDT.

INTRODUCTION

In a recent report, Peng *et al.* (1) reviewed the current literature and concluded that little is known about the details of localization patterns of photosensitizers used for photodynamic therapy (PDT). † Drug localization both *in vivo* and in culture was considered; the former representing a much more complex situation because partition of drugs to vasculature, stroma and host organs must be considered, as well as affinity of sensitizers, agents for plasma carriers that affect biodistribution (2).

Our approach to the question of sensitizer localization and its role in PDT efficacy began with an examination of localization of different sensitizers in cell culture. We assessed both sites of drug localization and site of photodamage detected using a series of fluorescent probes (3–6). This work was designed to evaluate the hypothesis that the site of photodamage was an important determinant of photodynamic efficacy. Based on reports showing that PDT sometimes did and sometimes did not yield an apoptotic response (7–9), we initiated a study designed to examine the possibility that the response to PDT was related

*To whom correspondence should be addressed at: Department of Pharmacology, WSU School of Medicine, Detroit, MI 48201, USA. Fax: 313-577-6739, dhkessel@med.wayne.edu.

†*Abbreviations:* AO, acridine orange; CCD, charge-coupled device; FHS, Fisher's medium with HEPES replacing Na_2CO_3 and containing 10% horse serum; PFGE, pulsed-field gel electrophoresis; LD_{50}, reduction in cell viability by 50%; PDT, photodynamic therapy; R123, rhodamine 123; SnET2, tin etiopurpurin; SnOPA, tin octaethylpurpurin amidine; TDPH, trimethylamino diphenylhexatriene; THF, tetrahydrofuran.

to the intracellular site(s) of photodamage. In previous studies, diverse sensitizers were employed, varying in structure, hydrophobicity, charge distribution and other physical properties that could affect direct comparisons. In the present study, we have examined the properties of two close drug analogs and present a hypothesis concerning factors that may determine the cellular response to PDT.

MATERIALS AND METHODS

Chemicals

(SnET2) etiopurpurin was provided by Dr. Alan Morgan, Department of Chemistry, University of Toledo, and from Dr. Chang's laboratory. The synthesis of tin octaethylpurpurin amidine (SnOPA) is described in the Appendix. Drug structures and absorbance spectra are shown in Fig. 1. The fluorescent probes HO342, acridine orange (AO), trimethylamino diphenylhexatriene (TDPH) and rhodamine 123 (R123) were obtained from Molecular Probes, Eugene, OR.

Tissue culture

The P388 cells were grown in Fischer's medium (GIBCO-BRL, Grand Island, NY) supplemented with 10% horse serum. Cells were used in the log phase of growth. Experiments were carried out using a HEPES-buffered formulation of Fischer's medium containing 10% horse serum termed FHS.

Distribution ratios

Cells (2×10^6/mL) were incubated with different levels of SnET2 or SnOPA, ranging from 1 to 10 μ*M* for 15 min at 37°C. Steady-state intracellular levels were achieved at this time. The cells were collected by centrifugation and the washed pellets dispersed in 3 mL of 10 m*M* Triton X-100 detergent. A 100 μL sample of the medium was similarly diluted into detergent. Triton-solubilized cells and media were excited with broadband light (390–450 nm) and the resulting fluorescence emission spectrum was acquired using an Instaspec IV charge-coupled device (CCD) array (Oriel Corp., Stamford, CT). A 550 nm high-pass filter was inserted into the emission beam to minimize interference by exciting light. Fluorescence at 670 nm was determined, corrected for the fluorescence of control (drug-free) samples and compared with a standard fluorescence-intensity curve prepared with SnET2 and SnOPA soyorrhexis and ultimately to massive necrotic areas. The actual basis for individual cell death at later times was obstructed by the extent of necrosis. The typical DNA ladder fragmentation pattern did agree with the cytopathologic results. Fragmentation of DNA to nucleosomes and nucleosome multimers was detected by static gel electrophoresis 8 h after PDT.

The *in vitro* incorporation of PCI-0123 within EMT6 cells increased with time. An incubation concentration of 20 μg/mL of PCI-0123 resulted in a retention level of 0.25 μmol/g protein at 2 h compared to 2.07 μmol/g protein at 40 h. The sensitizer was found to localize within lysosomes as detected by confocal microscopy. Ensuing photoillumination led to lysosomal rupture, extensive blebbing of the membranes and eventual cell death. The PCI-0123 is a cationic sensitizer (charge due to the lutetium metal) and, although other

cationic porphyrins (peripheral charge) have been shown to target mitochondria (11), some that are lipophilic and cationic do in fact target the lysosome (12). Lysosomes are an important subcellular PDT target.

Lysosomes are the primary site of intra- and extracellular digestion and are also involved in protein turnover and tissue remodelling. They are organelles containing hydrolytic enzymes that have an acidic pH optimum. Under normal physiological conditions lysosomal enzyme action is restricted to the interior of the cell. However, when tissue hyperacidification occurs, as in tumor tissue, lysosomal enzymes are activated to a greater extent due to their acidic pH optimum and attack the surrounding tissue (22). The relevance of porphyrin uptake into lysosomes and subsequent photosensitization leading to cell death have been studied by Allison *et al.* (23). Once the lysosomes are ruptured, cytoplasmic liberation of enzymes take place and cell death ensues. Lysosomes play a key role in the invasion of normal tissue by tumor cells (24, 25). Therefore it is highly reasonable to target substrates to lysosomes of tumor tissue as an effective method of tumor treatment because the activity of lysosomal enzymes is increased at the lower pH values present in tumoral tissues. Upon activation of lysosomal enzymes, cytolytic chain reactions ensue, leading to greater tumor destruction (22).

The PCI-0123 has an appreciable molar extinction coefficient at the far red-activated wavelength, thereby increasing tissue penetration and tumor destruction over many other photosensitizers (26). Lutetium texaphyrin localizes in tumor lesions; subsequent light irradiation induces selective tumoricidal effects without damage to normal tissues. The sensitizer's inherent fluorescent characteristics coupled with spectral bioimaging technology allowed for the noninvasive discernment and monitoring of tumor lesions before, during and after PDT. Photodynamic therapy induced an apoptotic response in the tumor lesions. The sensitizer was intracellularly localized within lysosomes, with photoirradiation leadlutions of known concentration. The distribution ratio is defined as the concentration of drug in the intracellular/extracellular fluid.

PDT

The P388 cells (2×10^6/mL) were incubated with 2 μ*M* SnET2 or 8 μ*M* SnOPA for 15 min at 37°C, then collected by centrifugation, taken up in cold FHS and irradiated at 10°C. The drug concentration was based on distribution ratio results, so that the intracellular sensitizer level was the same for both agents. The light source was a 600 W quartz–halogen lamp with IR radiation attenuated by a 700 nm cut-off filter and a 10 cm layer of water; the bandwidth was further defined by a 610 nm cut-off filter. The total power output at 610–700 nm, measured with an EGG model 450 photometer, was 5 mW cm^{-2} (light doses = 1.5 J cm^{-2}). In separate experiments, we ascertained that these PDT doses resulted in a 50% loss of viability. The latter was measured by observing cell growth with a Coulter electronic particle counter over a period of 3 days, during which time a control cell culture will increase eight-fold in density. We have observed that this approach yields results that do not significantly differ from clonogenic assays.

Detection of photodamage by fluorescent probes

Directly after irradiation, 2×10^6 control or photodamaged cells were incubated for 5 min at 37°C in FHS containing 1 μ*M* TDPH, 0.5 μ*M* AO or 10 μ*M* R123, then resuspended in 25 μL of FHS at 4°C for analysis of dye distribution by fluorescence microscopy. These probes detect membrane, lysosomal and mitochondrial photodamage, respectively, when used with the proper emission and excitation filters (4–6). Images were acquired using a digital CCD camera (Photometrics, Tucson, AZ), and processed with MetaMorph software (Universal Imaging Corp., West Chester, PA).

Detection of apoptosis by fluorescence microscopy

After irradiation, cell suspensions were diluted with FHS to a density of 4×10^5/mL, to prevent spontaneous apoptosis that can occur at high cell densities and held at 37°C for varying intervals. Control and irradiated cells were then collected and labeled with 2 μ*M* HO342 for 5 min at 37°C. Fluorescent nuclei were visualized using a Nikon Labophot fluorescence microscope (excitation = 330–380 nm, emission = 400–500 nm). Apoptotic nuclei show either sharp zones of bright fluorescence, representing condensed chromatin, or distinct patterns of fluorescent "dots," indicating fragmented chromatin. Numbers of apoptotic nuclei per field of 100 cells were scored in five separate fields. To obtain detailed fluorescent images, we used a 100X Nikon objective with an iris diaphragm.

Static gel electrophoresis

Cell pellets were deproteinized with proteinase K, and the DNA was precipitated with cold ethanol. The DNA preparations were loaded onto 1.5% agarose gels and electrophoresed for approximately 3.5 h (2 V/cm gradient). A molecular weight marker preparation (kit VI, 154–2165 bp) was provided by Boehringer/Mannheim (mol. wt. marker kit VI). Gels were stained with ethidium bromide and fluorescence patterns of DNA ladders examined under 310 nm UV light.

Pulsed-field gel electrophoresis (PFGE)

Cells were washed with PBS at 4°C and resuspended in L buffer (10 m*M* Tris, 100 m*M* EDTA, 20 m*M* NaCI, pH 7.6). An equal volume of 1% low melting-point agarose in L buffer was added. Plugs were formed at 0°C and transferred to 1 mL of L buffer containing 1% Sarkosyl + 0.5 mg/mL proteinase K. After incubation for 24 h at 50°C, the plugs were washed three times in TE buffer (1 h each). Pulsed-field electrophoresis is carried out using 1% agarose gels in TBE buffer (3.6 m*M* Tris, pH 8, 3.6 m*M* boric acid and 0.08 mM EDTA) at 4°C. The switch time was linearly varied from 3 to 45 s forward, 1 to 15 s reverse, voltage = 180, using a linear ramp, for 20 h.

PDT efficacy in a murine tumor model

The PDT responsiveness was estimated using DBA/2 mice bearing 5 ± 0.5 mm diameter subcutaneous SMT-F tumors. Sensitizers were administered on day 0 to groups of six animals, and the tumor sites were irradiated with 660 nm light (75 mW cm^{-2}, 135 J cm^{-2}) 24 h later. Numbers of animals with nonpalpable tumors were determined on days 7 and 10

after PDT. Based on drug absorbance at 660 nm, administered doses were 2.0 mg/kg of SnET2 and 4.3 mg/kg of SnOPA.

RESULTS

Transport studies indicated a distribution ratio of 9.1 ± 1.1 for SnET2 and 2.2 ± 1.3 for SnOPA, using extracellular drug concentrations that were varied between 1 and 10 μ*M*. These results indicate that the intracellular level of SnET2 will be approximately four-fold greater for SnOPA when equimolar levels of the drugs are used. A comparison of absorbance spectra (Fig. 1) indicates very nearly equal total absorbance (area under the curve) between 610 and 700 nm, the bandwidth of irradiation used in our *in vitro* PDT studies. We found that equitoxic effects on cell viability were achieved by incubating cells with 2 μ*M* SnET2 or 8 μ*M* SnOPA, then irradiating as described above.

A comparison of sites of localization of SnET2 and the analog SnOPA is shown in Fig. 2. Cells incubated with SnOPA showed a diffuse cytoplasmic fluorescence (Fig. 2A). In contrast, SnET2 was confined to discrete intracellular loci (Fig. 2D). Control cultures of P388 cells showed < 1 % apoptotic cells, using H0342 staining. When P388 cells were treated with an LD_{50} PDT dose of SnOPA, we observed no changes in the nuclear structure after 1 h (Fig. 2B) and <3% apoptotic cells. Apoptotic nuclei were observed 24 h times showed an apoptotic response, including endonucleosomal cleavage and formation of DNA ladders. In this context, we had reported that two cationic porphyrins that catalyzed membrane photodamage failed to produce an apoptotic response (10). These reports suggest that photosensitizers that partition to membrane loci and mediate membrane photodamage may evoke a necrotic, rather than an apoptotic response.

In the present study, we examined the effects of two sensitizers of related structure that vary in their localization patterns. In cell culture, SnET2 mediated photodamage to lysosomes and mitochondria but spared membranes. In contrast, the amidine analog SnOPA targeted lysosomes, mitochondria and membranes. This difference was associated with a substantial alteration in the expression of PDT-induced apoptosis. With SnET2, apoptotic chromatin was detected within 60 min after PDT; this effect was not observed until 24 h after PDT with SnOPA (Fig. 2). Data shown in Fig. 4 confirm that progression of DNA fragmentation was much slower after SnOPA photodamage, compared with the rapid appearance of 50 kbp DNA after PDT with SnET2. Results shown in Fig. 2I indicate that endonucleosomal DNA fragmentation was delayed, not abolished.

Data shown in Table 1 suggest that SnOPA is not significantly inferior to SnET2 *in vivo*, in spite of the differences in the rate of apoptotic response, but caution needs to be used in interpreting these data because a different cell line was used for the animal studies. The P388 tumor rapidly metastasizes to the lung in recipient animals, and its growth cannot be controlled by PDT.

The foregoing data are consistent with the hypothesis that membrane photodamage can lead to delayed (SnOPA) or arrested (high-dose Photofrin) apoptosis or to no apoptosis (cationic porphyrins). The variability may relate to the extent of photodamage and the resulting

leakiness of cell membranes. The determinants of apoptosis are, however, more complex than these results suggest. A porphycene dimer that caused photodamage to lysosomes, membranes and mitochondria elicited a rapid apoptotic response (13). Perhaps an explanation lies in the nature of the cell membrane, which is more than a barrier between the cell and its environment. Recent reports (14,15) indicate that membrane photodamage can yield a variety of effects. The membrane contains diverse receptors, transport systems and signal-transduction pathways, and the use of TDPH permeability measurements only characterizes membrane permeability changes. Detailed studies on the nature of photodamage produced by different photosensitizing agents will be needed to evaluate the role of membrane and other alterations as determinants of the apoptotic response to PDT.

Acknowledgments

This work was supported by grant CA 23378 from the National Cancer Institute, NIH, DHHS. We thank Ann Marie Santiago and Veronique Patacsil for excellent technical assistance. We thank Dr. T. J. Dougherty (Roswell Park Cancer Institute) for data on the *in vivo* response of the SMT-F tumors to PDT with SnET2 and SnOPA.

References

1. Peng Q, Moan J, Nesland JM. Correlation of subcellular and intratumoral photosensitizer localization with ul- trastructural features after photodynamic therapy. Ultrastruct Pathol. 1996; 20:109–129. [PubMed: 8882357]
2. Moan J, Berg K. Photochemotherapy of cancer: experimental research. Photochem Photobiol. 1992; 55:931–948. [PubMed: 1409894]
3. Kessel D. Characterization of photodynamic and sono-dynamic cytotoxicity by fluorescent probes. Proc SPIE. 1993; 1881:275–284.
4. Kessel D, Woodburn K, Henderson BW, Chang CK. Sites of photodamage *in vivo* and *in vitro* by a cationic porphyrin. Photochem Photobiol. 1995; 62:875–881. [PubMed: 8570726]
5. Kessel D, Woodburn K. Photosensitization with benzochlorin iminium salts. Proc SPIE. 1994; 2133:77–83.
6. Kessel D. Use of fluorescent probes for characterizing sites of photodamage. The Spectrum. 1993; 6:1–6.
7. Agarwal ML, Clay ME, Harvey EJ, Evans HH, Antunez AR, Oleinick NL. Photodynamic therapy induces rapid cell death by apoptosis in L5178Y mouse lymphoma cells. Cancer Res. 1991; 51:5993–5996. [PubMed: 1933862]
8. He XY, Sikes R, Thomsen S, Chung LWK, Jacques SL. Photodynamic therapy with Photofrin II induces programmed cell death in carcinoma cell lines. Photochem Photobiol. 1994; 59:468–473. [PubMed: 8022890]
9. Zaidi SIA, Oleinick NL, Zaim MT, Mukhtar H. Apoptosis during photodynamic therapy-induced ablation of RIF-1 tumors in C3H mice: electron microscopic, histopathologic and biochemical evidence. Photochem Photobiol. 1993; 58:771–776. [PubMed: 8309997]
10. Luo Y, Chang CK, Kessel D. Rapid initiation of apoptosis by photodynamic therapy. Photochem Photobiol. 1996; 63:528–534. [PubMed: 8934765]
11. Henderson BW, Dougherty TJ. How does photodynamic therapy work? Photochem Photobiol. 1992; 55:145–157. [PubMed: 1603846]
12. Dellinger M. Apoptosis or necrosis following Photofrin photosensitization: influence of the incubation protocol. Photochem Photobiol. 1996; 64:182–187. [PubMed: 8787012]
13. Kessel D, Luo Y, Woodburn K, Chang CK, Henderson BW. Mechanisms of phototoxicity catalyzed by two porphycenes. Proc SPIE. 1995; 2392:122–128.
14. Kochevar I, Lambert C, Lynch M, Tedesco A. Comparison of photosensitized plasma membrane damage caused by singlet oxygen and free radicals. Biochim Biophys Acta. 1996; 1280:223–230. [PubMed: 8639697]

15. Kochevar IE, Bouvier J, Lynch M, Lin CW. Influence of dye and protein location on photosensitization of the plasma membrane. Biochim Biophys Acta. 1994; 1196:172–180. [PubMed: 7841181]
16. Morgan AR, Tertel NC. Observations on the synthesis and spectroscopic characteristics of purpurins. J Org Chem. 1986; 51:1347–1349.
17. Kirby JP, van Dantzig NA, Chang CK, Nocera DG. Formation of porphyrin donor-acceptor complexes via an amidinium–carboxylale salt bridge. Tetrahedron Lett. 1995; 36:3477–3481.

APPENDIX

Synthesis of SnOPA

Diethyl cyanomethylphosphonate (1 g, 5.65 mmol) was added dropwise to a solution of NaH (0.24 g, 60% dispersion in mineral oil) in dry tetrahydrofuran (THF, 10 mL). To this mixture was added 1 g of 1.62 mmol Ni(II) meso-formyloc-taethylporphyrin (16) dissolved in THF (20 mL). The mixture was heated to reflux under nitrogen atmosphere for 1 h. Upon cooling, CH_2Cl_2 (250 mL) was added and the solution was washed three times with water in a separatory funnel and the organic layer was collected, dried with sodium sulfate and the solvent was removed *in vacuo*. The residue was column chromatographed on silica gel using a 1:1 mixture of CH_2Cl_2/hexane for elution to yield the nickel complex of the cyanoethenyl product (0.91 g, 1.48 mmol); MS m/e 641 (M +). This complex (500 mg, 0.78 mmol) was dissolved in CH_2Cl_2 (80 ml) and concentrated sulfuric acid (15 mL) was added with stirring. Stirring was continued until the upper organic layer became almost colorless. Ice (50 g) was added, followed by a saturated sodium carbonate solution. After neutralization, the organic layer was separated, washed with water and evaporated. A pure preparation of meso-(2-cyanoethenyl)octaethylporphyrin was obtained by crystallization from CH_2Cl_2/methanol in quantitative yield (450 mg). Ultraviolet-visible λ_{max} 406, 505, 539, 575, 626 nm; ^{1}H-NMR ($CDCl_3$,) d 10.06 (d, J = 17 Hz, 1 H, vinyl), 10.04 (s, 2 H, meso), 9.96 (s, 1 H, meso), 5.58 (d, J = 17 Hz, 1 H, vinyl), 3.99 (m, 16 H, ethyl), 1.80 (m, 24 H, ethyl), −3.14 (br s, 2 H, NH); MS m/e 585 (M +).

A solution of the cyanoethenylporphyrin (450 mg, 0.78 mmol) in glacial acetic acid (80 mL) was heated to reflux under N_2 for 24 h. The solvent was then removed *in vacuo* and the residue purified by column chromatography on silica gel using CH_2Cl_2 as solvent. A major green fraction was isolated and the cyano-octaethylpurpurin was crystallized from CH_2Cl_2–methanol to yield 368 mg (81%). Ultraviolet–visible λ_{max} 426, 523, 564, 635, 692 nm; ^{1}H-NMR ($CDCl_3$) d 9.51, 9.48, 8.49 (s, 1 H each, meso), 9.20 (s, 1 H, exocyclic ring), 3.80 (m. 12 H, ethyl), 2.95, 2.50 (m, 2 H each, ethyl), 1.75 (m. 24 H, ethyl), −0.10, −1.05 (s, 1 H each, NH); MS m/e 585 (M +).

Tin (IV) octaethylpurpurin amidinium salt

Tin (II) chloride (70 mg) and sodium acetate (20 mg) were added to a solution of cyano-octaethylpurpurin (50 mg, 0.085 mmol) in acetic acid (15 mL), and the mixture was heated to reflux until metal insertion was complete (4 h, monitored by UV and TLC). The resulting mixture was then partitioned between CH_2Cl_2 and water. The organic layer was separated and evaporated to give the Sn(IV) complex of cyano-octaethylpurpurin, which was further chromatographed on silica gel, eluting with 15% methanol in CH_2Cl_2. The yield was 35 mg

(50%); UV–visible λ_{max} 436, 540, 615, 659 nm. This complex was placed in a Schlenck tube with dry toluene (20 mL). After the system was deaerated, 1 mL of 1 *M* toluene solution of methyl chloroaluminum amide (17) was introduced through a syringe. The mixture was stirred at 80°C for 3 days under argon atmosphere. The solvent was then evaporated and the residue was dissolved in CH_2Cl_2, washed with 0.1 *N* HCl and filtered. Evaporation of the solvent gave the amidinium salt SnOPA (25 mg, 81% yield); UV–visible λ_{max} 429, 455, 602, 640, 670 nm; FAB-MS m/e 788 for $C_{29}H_{49}N_6SnCl_2$.

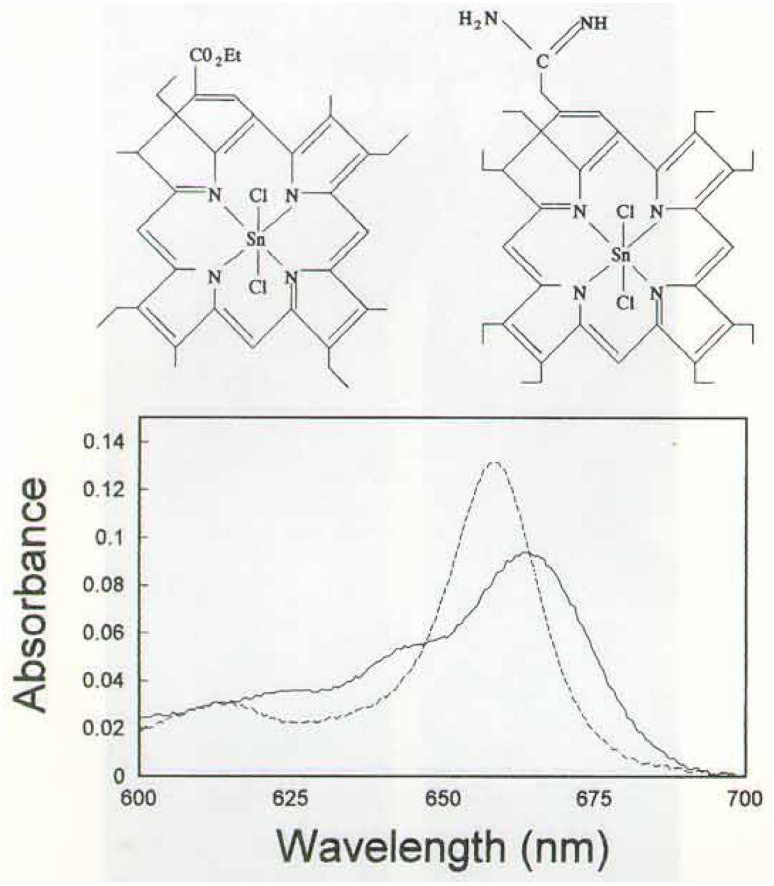

Figure 1.

Top: structures of SnET2 (left) and SnOPA (right). Bottom: absorbance spectra of SnET2 (dashed line) and SnOPA (solid line) between 600 and 700 nm.

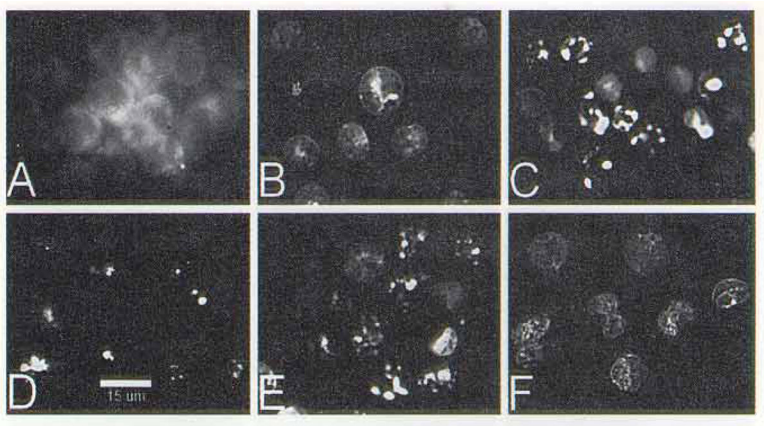

Figure 2.

Localization of SnOPA (A) and SnET2 (D); resulting patterns of nuclear apoptotic response (detected by HO342 staining) at 1 and 24 h after LD_{50} PDT doses with SnOPA (1 h = B, 24 h = C) and SnET2 (1 h = C. 24 h = F). The white bar at the bottom of panel D = 15 μm.

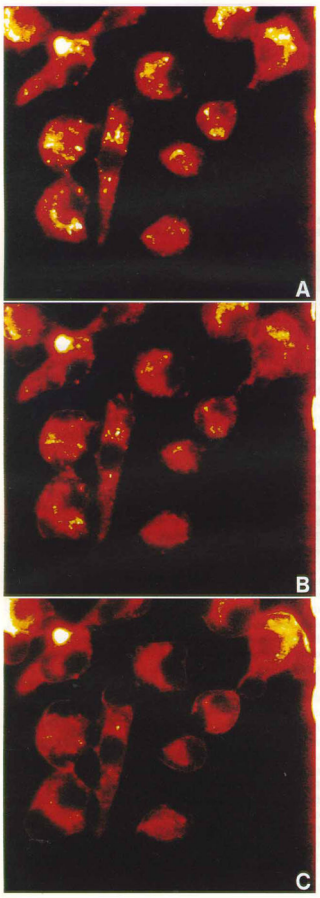

Figure 5.

In vitro subcellular localization of PCI-0123 in EMT6 cells for 4 h (a) with the subsequent effects of photoirradiation (b, c). Cells were exposed to sequential scans of 2.0 s of light followed by 5.5 s delays. (b, c) After 20 and 80 scans, which equate to 40 and 160 s of irradiation, respectively.